Design approach for post-buckled beams in bistable piezoelectric energy harvesters

Aya Benhemou, Thomas Huguet, David Gibus, Aurélien Carré, Camille Saint-Martin, Émile Roux, Ludovic Charleux, Adrien Morel, Adrien Badel

▶ **To cite this version:**

Aya Benhemou, Thomas Huguet, David Gibus, Aurélien Carré, Camille Saint-Martin, et al.. Design approach for post-buckled beams in bistable piezoelectric energy harvesters. IEEE Wireless Power Week (WPW 2022), Jul 2022, Bordeaux, France. pp.136-140, 10.1109/WPW54272.2022.9853996 . hal-03780330

HAL Id: hal-03780330
https://hal.science/hal-03780330

Submitted on 19 Sep 2022

HAL is a multi-disciplinary open access archive for the deposit and dissemination of scientific research documents, whether they are published or not. The documents may come from teaching and research institutions in France or abroad, or from public or private research centers.

L'archive ouverte pluridisciplinaire **HAL**, est destinée au dépôt et à la diffusion de documents scientifiques de niveau recherche, publiés ou non, émanant des établissements d'enseignement et de recherche français ou étrangers, des laboratoires publics ou privés.

Design approach for post-buckled beams in bistable piezoelectric energy harvesters

Aya BENHEMOU
SYMME
Univ. Savoie Mont-Blanc
F-74000, Annecy, France
aya.benhemou@univ-smb.fr

Thomas HUGUET
LAPLACE
Université de Toulouse, CNRS, INPT
F-31071 Toulouse, France
Thomas.huguet@toulouse-inp.fr

David GIBUS
SYMME
Univ. Savoie Mont-Blanc
F-74000, Annecy, France
david.gibus@univ-smb.fr

Aurélien CARRE
SYMME
Univ. Savoie Mont-Blanc
F-74000, Annecy, France
aurelien.carre@univ-smb.fr

Camille SAINT-MARTIN
SYMME
Univ. Savoie Mont-Blanc
F-74000, Annecy, France
camille.saint-martin@univ-smb.fr

Emile ROUX
SYMME
Univ. Savoie Mont-Blanc
F-74000, Annecy, France
emile.roux @univ-smb.fr

Ludovic CHARLEUX
SYMME
Univ. Savoie Mont-Blanc
F-74000, Annecy, France
ludovic.charleux @univ-smb.fr

Adrien MOREL
SYMME
Univ. Savoie Mont-Blanc
F-74000, Annecy, France
adrien.morel @univ-smb.fr

Adrien BADEL
SYMME
Univ. Savoie Mont-Blanc
F-74000, Annecy, France
adrien.badel @univ-smb.fr

***Abstract* — This paper presents a model suited for the design of mechanically bistable beams used in Piezoelectric Energy Harvesters (PEHs). The proposed model accounts for the bending and compression of post-buckled beams used in the PEH. The effect of the beam's geometry on the generated power and frequency bandwidth is evaluated with a performance criterion. It is concluded that a low beam compression stiffness can have a negative impact on the performance of the PEH and that the bending stiffness solely implies a prestress on the piezoelectric transducer.**

Keywords— Piezoelectric energy harvester, bistable, post-buckled beams, lumped model, design

I. Introduction

Piezoelectric Energy Harvesters (PEHs) have received a lot of attention in recent years as they offer a promising cost-effective, durable and autonomous alternative to chemical batteries for powering wireless sensor networks [1]. To improve the performance of a PEH subjected to ambient vibrations, a wider frequency bandwidth is preferred. For that matter, non-linear vibrating structures in PEHs have become a technology of interest in the past 2 decades [2].

Bistability is one example of non-linearity used in these types of power generators that has been extensively studied [3]; it implies the existence of two stable equilibrium positions in the structure. Other than magnetic interaction based structures [4], bistability can be realized with post-buckled structures such as beams [5]. This type of mechanical non-linearity implies considerable modelling complexity regarding the dynamic behavior of the beams.

Consequently, the effect of the beams is omitted in the Duffing type equations used to describe bistable PEHs for some architectures [6].

Nevertheless, the static behavior of thin beams post-buckling has been modelled extensively. In 1998, Vangbo et al. proposed a static Lagrangian approach to study post-buckled beams with a centered actuation [7] that has been used by many, including Camescasse et al. who investigated the effect of off-center actuation, amongst other elements, on the static behavior of post-buckled beams in 2013 [8].

This modelling strategy was widely employed to develop lumped models for dynamic structures that use post-buckled beams. A dynamic lumped model for a tunable MEMS architecture was developed and verified experimentally by Saif in the year 2000 [9] who used this method, but only modelled the mechanical behavior of the post-buckled beams as the effect of the electrical part of the structure was omitted in his work.

Regarding energy harvesting applications, a considerable contribution to the study of post-buckled beams for PEH's was made by Cottone et al in 2012, who modelled the behavior of post-buckled membranes [10] and took both mechanical and electrical parts of the structure into consideration. The effect of post-buckled beams is however difficult to assess in the proposed model due to the

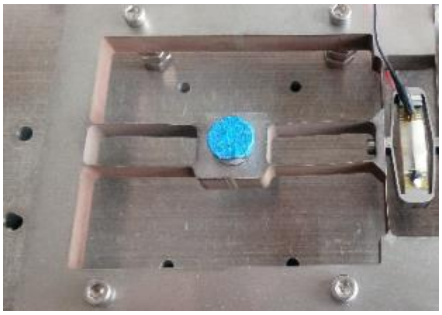

Fig. 1 The bistable PEH studied by Huguet [6]

complexity and additional non-linearity of the terms involved. It can thus be costly and complicated to draw general conclusions regarding the geometry's effect on the dynamic performance of the generator, especially for structures that use the piezoelectric element differently. It is also worth citing Liu et al [11] who considered the bending stiffness of the beams in a dynamic lumped model for design purposes, proving that the latter had no effect on the generated power and frequency bandwidth obtained by the PEH for the architecture investigated. However, the effect of the compression stiffness of the post-buckled beams on the performance of the PEH remains undetermined.

This paper proposes a modelling approach for this purpose, that combines static Finite Element Analysis (FEA) with a dynamic lumped model, allowing the study of the effect of the bending and compression stiffnesses of post-buckled beams with complex geometries on the performance of a bistable PEH.

II. LUMPED MODEL FOR A MECHANICALLY BISTABLE PEH ARCHITECTURE

A. Presentation of the PEH architecture studied

The PEH architecture studied in this paper is similar to Huguet's PEH prototype described in [6] and represented in *Fig. 1*.

It includes an inertial mass, four bistable thin beams used to prevent in plan rotations of the inertial mass, and an Amplified Piezoelectric Actuator (or APA) used to generate power upon the inertial mass's movement.

The advantage of using this type of architecture is the exploitation of 3-3 electromechanical coupling modes in the piezoelectric element as opposed to the 3-1 electromechanical coupling modes that are usually solicited in PEH architectures that use piezoelectric patches [10].

B. Lumped model formulation for the studied PEH architecture

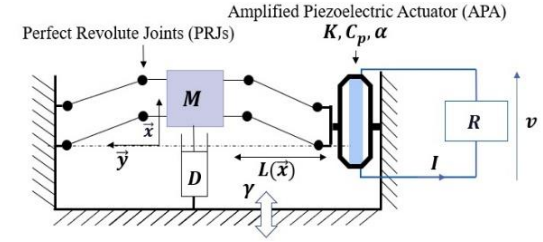

Fig. 2 A representation of the classic bistable PEH's lumped model

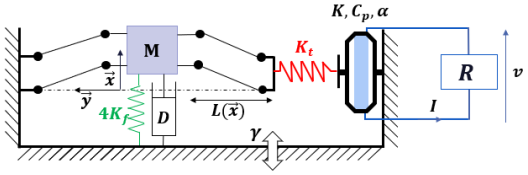

Fig. 3 A representation of the proposed bistable PEH's lumped model

In Fig. 2, a schematic of the classic modelling approach for the studied architecture is shown. The bistable beams are usually considered to be Perfect Revolute Joints (PRJs) with infinitely rigid bars.

In reality, the bistable beams are subject to mechanical strain during the inertial mass's movement; mainly bending strain modes and extension/compression strain modes.

Fig. 3 is a schematic of the modelling approach proposed in this paper for mechanically bistable PEHs, in which the elasticity of the bistable beams is considered by adding springs for their bending and compression stiffnesses respectively named K_f and K_t. The bending stiffnesses of the four identical links act in parallel on the mass and oppose its displacement along the x direction. They can thus be modelled with an equivalent stiffness $4K_f$. The compression stiffnesses oppose the mass's movement along the $\vec{y}$ direction.

Along this axis the compression stiffnesses of the links add up on both sides of the mass, but are in series when considering both sides. The global equivalent compression stiffness K_t is then equal to the compression stiffness of one beam.

The inertial mass is considered moving along the $\vec{x}$ direction only (which is true to the first order if the position of the mass x is very small compared to the length of the links L).

To simplify the modelling process, the APA (K, α) and the buckled links' compression spring (K_t) are modelled with an equivalent APA (K_{eq}, α_{eq}).

The expression of the force applied by the APA and the buckled link's compression spring becomes:

$$K_{eq} = \frac{K_{APA}}{K_t + K_{APA}} \tag{1}$$

$$\alpha_{eq} = \frac{\alpha}{K_t + K_{APA}} \tag{2}$$

Dynamic equilibrium equations of the PEH represented in Fig. 3 can be deduced by formulating the Euler-Lagrange equations for the system.

The displacement of the equivalent APA is expressed as follows:

$$\Delta L = 2(L(\vec{x}) - L) = \left(2L - 2\sqrt{L^2 + x_0^2 - x^2}\right) \tag{3}$$

The generalized coordinates considered are the position of the mass x and a voltage related coordinate λ as $\dot{\lambda} = V$. The Euler-Lagrange system of equations is formulated as follows:

$$\begin{cases} M\gamma = \dfrac{d}{dt}\left(\dfrac{\partial L}{\partial \dot{x}}\right) - \dfrac{\partial L}{\partial x} \\ I = \dfrac{d}{dt}\left(\dfrac{\partial L}{\partial \dot{\lambda}}\right) - \dfrac{\partial L}{\partial \lambda} \end{cases} \tag{4}$$

The Lagrangian function of the system is described by the equation below:

$$L = T - S_{4K_f} - S_{K_{eq}} + W_c \tag{5}$$

With:

$$T = \frac{1}{2} M \dot{x}^2 \tag{6}$$

$$S_{K_{eq}} = 2\left(\frac{1}{2} K_{eq} \Delta L^2\right) \tag{7}$$

$$S_{K_f} = \frac{1}{2}\left(4K_f x^2\right) \tag{8}$$

$$W_c = \frac{1}{2} C_p v^2 + \alpha v \Delta L \quad (9)$$

The final equations that stem from the simplification of previous expressions are described in the equation system below:

$$\begin{cases} M\gamma = M\ddot{x} + 2K_{eq}\left(2L - 2\sqrt{L^2 + x_0^2 - x^2}\right)\frac{x}{\sqrt{L^2 + x_0^2 - x^2}} \\ \quad + 4\,K_f\,x + D\dot{x} + \\ \quad 2\alpha_{eq} v\, tg(\theta) + \frac{2\,\alpha_{eq}\,v\,x}{\sqrt{L^2 + x_0^2 - x^2}} \\ \quad I = \frac{2\,\alpha\beta_{K_t} x\dot{x}}{L} - C_p\dot{v} \end{cases} \quad (10)$$

Consequently, the behavior of the PEH can be described by the following equation system, provided the displacements of the mass and buckling level are small with respect to L ($x_0 << L$ et $x << L$):

$$\begin{cases} M\gamma = M\ddot{x} - \left(2K\beta_{K_t}\frac{x_0^2}{L^2} - 4K_f\right)x \\ \quad + \frac{2K\beta_{K_t}x^3}{L^2} + D\dot{x} + \frac{2\alpha\beta_{K_t}xv}{L} \\ \quad I = \frac{2\,\alpha\beta_{K_t} x\dot{x}}{L} - C_p\dot{v} \end{cases} \quad (11)$$

With β_{K_t} a correction factor that considers the effect of the compression stiffness and given by:

$$\beta_{K_t} = \left(\frac{1}{1 + \frac{K}{K_t}}\right) \quad (12)$$

When the buckled links' elasticity is not considered, the assumption of PRJs with infinitely rigid bars is made. It implies a null bending stiffness K_f and an infinite compression stiffness K_t (and thus a correction factor β_{K_t} equal to one). In this case, it is worthwhile noting that the equations describing the dynamic behavior of the harvester demonstrated by Huguet in [6] are obtained (see equation system (13)).

$$\begin{cases} M\gamma = M\ddot{x} - 2K\frac{x_0^2}{L^2}x + \frac{2K}{L^2}x^3 + D\dot{x} + \frac{2\alpha}{L}xv \\ I = \frac{2\alpha}{L}x\dot{x} - C_P\dot{v} \end{cases} \quad (13)$$

In an initial optimization based on the perfect revolute joint model, for a railway's application, the generator parameters specified in *Table 1* were set. The value of the load resistance is set to match the modulus of the output impedance of the harvester at the characteristic angular frequency ω_0:

$$R = \frac{1}{C_P\omega_0} \quad (15)$$

ω_0 being the resonance frequency of the bistable harvester for small oscillations around one of the two equilibrium positions.

$$\omega_0 = \frac{x_0}{L}\sqrt{\frac{4*K}{M}} \quad (16)$$

Table 1 The bistable PEH fixed parameters

Parameter	Symbol	Value
Mass frame distance	L	35 mm
Buckling level	x_0	0,85 mm
Inertial mass	M	5 g
APA stiffness	K	0,342 N/µm
Damping coefficient	D	0,026 N/m/s
Piezoelectric force factor	α	0,096 N/V
Piezoelectric clamped capacitance	C_P	1,55 µF
Load resistance	R	2,37 kΩ

Prior to determining the buckled beams' optimal geometry with the dynamic lumped model suggested in equations (11) the model's validity is tested by a comparison with a static finite element analysis.

III. A STATIC FINITE ELEMENT ANALYSIS OF POST BUCKLED BEAMS

The validity of the proposed lumped model is tested by comparing the elastic energy stored in the statically deformed buckled beams computed by Finite Element Analysis (FEA) $E_{b_{FEA}}$ with the elastic energy $E_{b_{LM}}$ calculated using the proposed lumped model described by (10) (11). The latter is given by equation (14).

$$E_{b_{LM}} = S_{K_f} + S_{K_t} = \frac{1}{2}K_f\,x^2 + \frac{K}{K_t}\,E_{APA} \quad (14)$$

With E_{APA} the elastic energy stored in the APA.

In order to validate the theoretical approach, beam dimensions are fixed as specified in Table 2.

Table 2 *Simulated buckled beam characteristics*

Buckled beam characteristics	Symbol	Value
Length	L	35 mm
Width	b	5 mm
Thickness	E	0,2 mm
Buckling level	x_0	0,85 mm

For simple beam geometries, such as straight section beams with a constant moment of inertia J, the bending and compression stiffnesses are known for a given material whose young modulus is E:

$$(K_f, K_t) = \left(\frac{96EJ}{(2L)^3}, \frac{Ebe}{L}\right) \quad (15)$$

The elastic energies S_{K_f}, S_{K_t} and $E_{b_{LM}}$ can then be calculated using equations (14) and (15) as a function of x. The elastic energy $E_{b_{FEA}}$ is numerically computed using the software Abaqus. The elastic energy $E_{b_{LM}}$ predicted by the lumped model and the FEA predictions $E_{b_{FEA}}$ are represented in Fig. 4 as well as the relative error between the $E_{b_{FEA}}$ and $E_{b_{LM}}$. The results show that the difference between the FEA and lumped model predictions is less than 10%, which confirms the soundness of the proposed approach.

It should be noted that for beams with more complex geometry than rectangular cross-section beams, K_f and K_t can be computed by static FEA and then used in the lumped model for dynamic simulations.

IV. THE EFFECT OF BISTABLE POST-BUCKLED STRUCTURES ON THE PERFORMANCE OF A PEH

A. Preliminary conclusions

Based on comparisons between the proposed dynamic lumped model (see equations (11)) and the classic lumped model based on the PRJ assumption with infinitely rigid bars

(see equations (13)), first conclusions on how the bending and compression stiffnesses of the links affect the PEH's behavior can be made.

The bending stiffness K_f affects the buckling level of the structure. This can be shown by rewriting the linear term in the mechanical part of the equation system (11).

$$\left(2K\beta_{K_t}\frac{x_0^2}{L^2} - 4K_f\right)x = \frac{2K\beta_{K_t}}{L^2}x_{01}^2 x \tag{16}$$

which leads to the expression of the new buckling level x_{01}:

$$x_{01} = \sqrt{\left(x_0^2 - \frac{2K_f L^2}{K\beta_{K_t}}\right)} \tag{17}$$

The equation system (11) can then be rewritten as:

$$\begin{cases} M\gamma = M\ddot{x} - \dfrac{2K\beta_{K_t}}{L^2}x_{01}^2 x + \dfrac{2K\beta_{K_t}x^3}{L^2} + D\dot{x} + \dfrac{2\alpha\beta_{K_t}xv}{L} \\ I = \dfrac{2\,\alpha\beta_{K_t}x\dot{x}}{L} - C_p\dot{v} \end{cases} \tag{18}$$

In reality, the same buckling level as the one set in the case of the perfect revolute joint assumption with infinitely and rigid bars (x_0 in equations (13)) can be established, provided that the force applied on the beams along the y direction, and consequently on the APA, is higher.

The bending stiffness K_f can be a seen as an indicator of the force necessary for buckling a given structure. The bigger it becomes, the more challenging it is to buckle the structure and move the mass (see equation (17)), and thus the beams, for an acceptable stress level fixed by the materials used for the links or by the displacement limit of the used APA. Consequently, the maximal value of the stiffness K_f should be considered to fix the limit of the design optimization domain. Comparing equations (18) and (13) we can finally note that K_f has no effect on the PEH's dynamic, since, for a given buckling level, the only difference comes from the stiffness K_t through the β_{K_t} parameter.

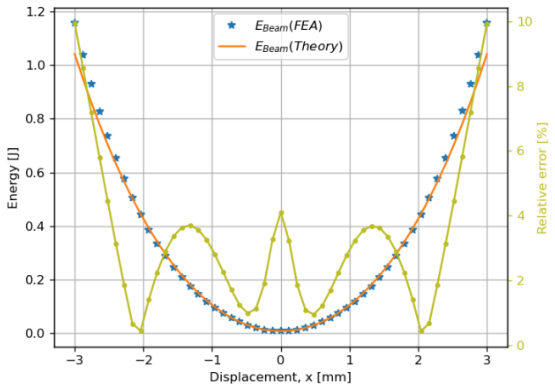

Fig. 4 Results for the FEA and lumped model for the elastic energy stored in a beam as a function of the mass displacement

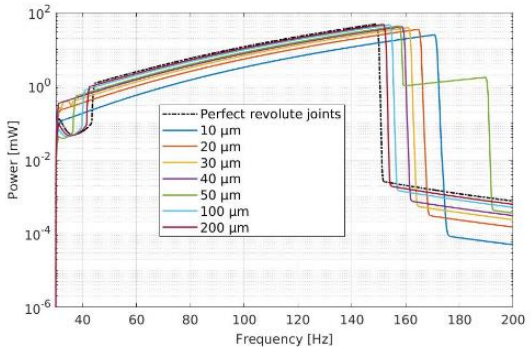

Fig. 5 Frequency responses for of the PEH for different beam thicknesses and for the PRJ with infinitely rigid bars

B. *Performance assessment of a bistable PEH*

Two physical values are usually considered to evaluate the performance of PEHs driven by sinusoidal vibrations: the generated power and the frequency bandwidth [3]. A unique metric can be used to assess both aspects for a given value of K_t. It consists in integrating the mean harvested power $P_{K_t}(f)$ along the frequency domain for a sinusoidal driving vibration of constant acceleration amplitude (see equation (19)).

$$I(K_t) = \int_{f_{min}}^{f_{max}} P_{K_t}(f)df \tag{19}$$

The performance criterion considered for the optimization of the flexible joints geometries is calculated as indicated in equation (20) as the previous metric (19) normalized by its value in the case of perfect revolute joints with infinitely rigid bars ($K_t \to +\infty$).

$$P_c(K_t) = \frac{I(P_{K_t})}{I(P_{K_t=\infty})} \tag{20}$$

C. *Optimization example: Optimal thickness of beams for a bistable PEH*

As an example, the performance criterion described by equation (18) is calculated for the beam described in Table 2 for different values of the beam thickness, and thus for different values of K_t (see equation (15)) for an ascending frequency sweep from 20 Hz to 200 Hz with an amplitude of 2g. The frequency varies linearly and its variation velocity is slow enough to consider quasi-static sinusoidal operation.

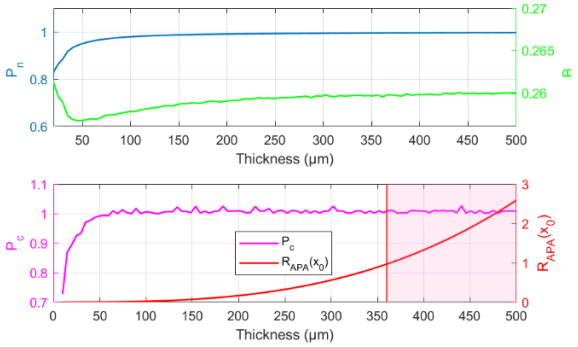

Fig. 6 Performance and feasibility assessments for different beam thicknesses

The frequency range and vibration level correspond to the targeted ambient vibration's spectrum in railways applications. To further understand the performance's evolution for different values of K_t ,normalized measures of power and bandwidth are calculated as follows:

$$P_n(K_t) = \frac{max\left(P_{K_t}(f)\right)}{max\left(P_{K_t=\infty}(f)\right)} \quad (21)$$

$$B_n(K_t) = \frac{\Delta f\left(P_{K_t} = \frac{max\left(P_{K_t}(f)\right)}{2}\right)}{f_c} \quad (22)$$

Furthermore, the ratio of the compression of the APA to its limit $R_{APA}(x_0)$ is evaluated for the fixed buckling level x_0 as a measure of feasibility. The APA used for energy generation is Cedrat Technologies' APA120S that has a displacement limit of 100 µm, and the lumped model parameters used for the dynamic numerical simulation are the ones specified in Table **1**.

The frequency response of the PEH for different beam thicknesses and for the PRJs with infinitely rigid bars shown in Fig. 5. The evolution of the bistable PEH's normalized power $P_n(K_t)$, normalized bandwidth $B_n(K_t)$ and performance criterion $P_c(K_t)$ are shown in Fig. 6 as functions of the beam's thickness. The evolution of the optimization criterion shows that the higher the thickness, and thus the compression stiffness *Kt*, the more the optimization criterion converges to 1.

It is worthy to note that the normalized power and bandwidth increase and decrease respectively with *Kt*, until reaching a constant level. The results agree with the evolution of the parameters of the model: the correction factor β_{K_t} approaches 1 as K_t increases, and consequently, the force factor of the APA approaches its optimal value as the compression elastic energy stored in the beams becomes negligible compared to that of the APA.

In addition, feasibility assessment results show that the normalized APA displacement exceeds one for a thickness larger than 360 µm, meaning that the generator is no longer feasible in the domain highlighted in red in Fig. 6. It is deduced that the compression stiffness offering the best performance can be attained starting a beam thickness of 200 µm, which corresponds to the optimal design.

V. Conclusion

In a nutshell, this paper proposes a modelling approach for the design of post-buckled beams in mechanically bistable PEH architectures.

The modelling approach is at first validated with a static FEA simulation, and then exploited for the evaluation of a performance criterion that accounts for the power output and frequency bandwidth.

As demonstrated in this work, the beam's bending stiffness has no effect on the performance of the PEH for this type of architecture, but is crucial to determine feasibility.

Additionally, the beam's compression stiffness is shown to deter the performance of the generator when its value becomes too small compared to the piezoelectric element's stiffness.

Therefore, a compromise between a rigid beam, for performance purposes, and a bendable beam, for feasibility purposes, should be found.

This approach can easily be applied to more complex post-buckled beams using static FEA simulations to determine the stiffnesses that correspond to bending and compression.

Experimental validations of the accuracy of the lumped model will soon be realized for simple and more complex beam geometries.

Acknowledgment

This project has received funding from the European Union's Horizon 2020 research and innovation program under grant agreement No 862289.

References

[1] M. Teresa Penella, J. Albesa, and M. Gasulla, 'Powering wireless sensor nodes: Primary batteries versus energy harvesting', in *2009 IEEE Intrumentation and Measurement Technology Conference*, Singapore. Singapore, May 2009, pp. 1625–1630. doi: 10.1109/IMTC.2009.5168715.

[2] M. F. Daqaq, R. Masana, A. Erturk, and D. Dane Quinn, 'On the Role of Nonlinearities in Vibratory Energy Harvesting: A Critical Review and Discussion', *Appl. Mech. Rev.*, vol. 66, no. 4, p. 040801, Jul. 2014, doi: 10.1115/1.4026278.

[3] R. L. Harne and K. W. Wang, 'A review of the recent research on vibration energy harvesting via bistable systems', *Smart Mater. Struct.*, vol. 22, no. 2, p. 023001, Feb. 2013, doi: 10.1088/0964-1726/22/2/023001.

[4] S. C. Stanton, C. C. McGehee, and B. P. Mann, 'Nonlinear dynamics for broadband energy harvesting: Investigation of a bistable piezoelectric inertial generator', *Phys. Nonlinear Phenom.*, vol. 239, no. 10, pp. 640–653, May 2010, doi: 10.1016/j.physd.2010.01.019.

[5] R. Masana and M. F. Daqaq, 'Energy harvesting in the super-harmonic frequency region of a twin-well oscillator', *J. Appl. Phys.*, vol. 111, no. 4, p. 044501, Feb. 2012, doi: 10.1063/1.3684579.

[6] T. Huguet, 'Vers une meilleure exploitation des dispositifs de récupération d'énergie vibratoire bistables : Analyse et utilisation de comportements originaux pour améliorer la bande passante', p. 180.

[7] M. Vangbo, 'An analytical analysis of a compressed bistable buckled beam', *Sens. Actuators Phys.*, vol. 69, no. 3, pp. 212–216, Sep. 1998, doi: 10.1016/S0924-4247(98)00097-1.

[8] B. Camescasse, A. Fernandes, and J. Pouget, 'Bistable buckled beam: Elastica modeling and analysis of static actuation', *Int. J. Solids Struct.*, vol. 50, no. 19, pp. 2881–2893, Sep. 2013, doi: 10.1016/j.ijsolstr.2013.05.005.

[9] M. T. A. Saif, 'On a tunable bistable MEMS-theory and experiment', *J. Microelectromechanical Syst.*, vol. 9, no. 2, pp. 157–170, Jun. 2000, doi: 10.1109/84.846696.

[10] F. Cottone, L. Gammaitoni, H. Vocca, M. Ferrari, and V. Ferrari, 'Piezoelectric buckled beams for random vibration energy harvesting', *Smart Mater. Struct.*, vol. 21, no. 3, p. 035021, Mar. 2012, doi: 10.1088/0964-1726/21/3/035021.

[11] W. Q. Liu, A. Badel, F. Formosa, Y. P. Wu, and A. Agbossou, 'Novel piezoelectric bistable oscillator architecture for wideband vibration energy harvesting', *Smart Mater. Struct.*, vol. 22, no. 3, p. 035013, Mar. 2013, doi: 10.1088/0964-1726/22/3/035013.